Organic & Biomolecular Chemistry

Cite this: *Org. Biomol. Chem.*, 2011, **9**, 3844

www.rsc.org/obc

PAPER

Highly selective fluorescent OFF–ON thiol probes based on dyads of BODIPY and potent intramolecular electron sink 2,4-dinitrobenzenesulfonyl subunits†

Huimin Guo,*[a] Yingying Jing,[a] Xiaolin Yuan,[b] Shaomin Ji,[a] Jianzhang Zhao,*[a] Xiaohuan Li[b] and Yanyan Kan[c]

Received 20th October 2010, Accepted 15th December 2010
DOI: 10.1039/c0ob00910e

Two highly selective OFF–ON green emitting fluorescent thiol probes (**1** and **2**) with intense absorption in the visible spectrum (molar extinction coefficient ε is up to 73 800 M^{-1} cm^{-1} at 509 nm) based on dyads of BODIPY (as electron donor of the photo-induced electron transfer, *i.e.*PET) and 2,4-dinitrobenzenesulfonyl (DNBS) (as electron acceptor of the PET process) were devised. The single crystal structures of the two probes were determined. The distance between the electron donor (BODIPY fluorophore) and the electron acceptor (DNBS) of probe **2** is larger than that of probe **1**, as a result the contrast ratio (or the PET efficiency) of probe **2** is smaller than that of probe **1**. However, fluorescence OFF–ON switching effects were observed for both probe **1** and probe **2** in the presence of cysteine (the emission enhancement is 300-fold for probe **1** and 54-fold for probe **2**). The fluorescence OFF–ON sensing mechanism is rationalized by DFT/TDDFT calculations. We demonstrated with DFT calculations that DNBS is *ca.* 0.76 eV more potent to accept electrons than the maleimide moiety. The probes were used for fluorescent imaging of cellular thiols.

Introduction

Thiols such as glutathione and cysteine play important roles in living organisms.[1–4] Thus, fluorescent molecular probes for selective detection of thiols are of great interest. A wide variety of fluorophores and sensing mechanisms have been used for design of fluorescent thiol molecular probes.[5] For fluorescent thiol probes, usually the fluorophores bear electrophilic groups (*e.g.*, iodoacetamides and benzyl halides), to which thiols may be covalently attached *via* electrophilic substitution. Alternatively fluorophores attached with a maleimide unit are also used as thiol probes.[6–8] Fluorophores containing a formyl (–CHO) group are also used for the construction of thiol probes, which are based on tuning the intramolecular charge transfer (ICT) effect. In this kind of probe, the –CHO group, as the electron acceptor of the ICT, can be transformed into a thiazolidine structure, which is electron-donating. Thus ratiometric as well as fluorescent OFF–ON signal transduction was observed in the presence of cysteine for these ICT-based probes.[5a,9]

A photo-induced electron transfer (PET) thiol probe with BODIPY as the fluorophore/electron donor and maleimide as the electron acceptor is particularly interesting (probe **3**, Scheme 1).[7] BODIPY is ideal for assembling molecular probes due to its characteristic photophysics, such as high fluorescence quantum yield (even in aqueous media), pH-independent emission, visible excitation/emission wavelength and excellent photostability, *etc.*[10–14] On the other hand, maleimide is well-established as an electron acceptor for the construction of PET thiol probes.[5] It was supposed that the C=C double bond of maleimide serves as an electron acceptor to quench the emission of the fluorophore, thus the probe is non-fluorescent. 1,4-Michael addition with thiols will saturate the C=C double bond of the maleimide unit, thus the PET quenching effect is prohibited and the fluorescence of the fluorophore is switched on.[5,7] However, this explanation of the sensing mechanism is based on speculation, and to the best of our knowledge, the sensing mechanism has not been rationalized from a theoretical perspective.

However, the PET effect of probe **3** is narrowly effective; *i.e.* only the *ortho*-isomer (**3**) shows negligible background emission (Φ = 0.002, Scheme 1),[7] whereas the *m*- and *p*-isomers give significant background emission (*e.g.* Φ = 0.37 for probe **4** and Φ = 0.54 for probe **5**, Scheme 1), due to the poor PET effect of **4** and **5**.[7] Thus **4** and **5** *cannot* be used as *effective* thiol probes. The effective PET of probe **3** was attributed to the shorter distance between

[a]*State Key Laboratory of Fine Chemicals, School of Chemical Engineering, Dalian University of Technology, Dalian 116024, P. R. China. E-mail: zhaojzh@dlut.edu.cn, guohm@dlut.edu.cn*
[b]*Center Laboratory, Affiliated Zhongshan Hospital of Dalian University, Dalian 116001, P. R. China*
[c]*Department of Immunology, Harbin Medical University, 194 Xuefu Road, Harbin 150081, P. R. China*

† Electronic supplementary information (ESI) available: General experimental methods, ^1H and ^{13}C NMR spectra of the compounds, theoretical calculations details (z-matrix), theoretical rationalization of the PET effect of the probes. CCDC reference numbers 787588–787590. For ESI and crystallographic data in CIF or other electronic format see DOI: 10.1039/c0ob00910e

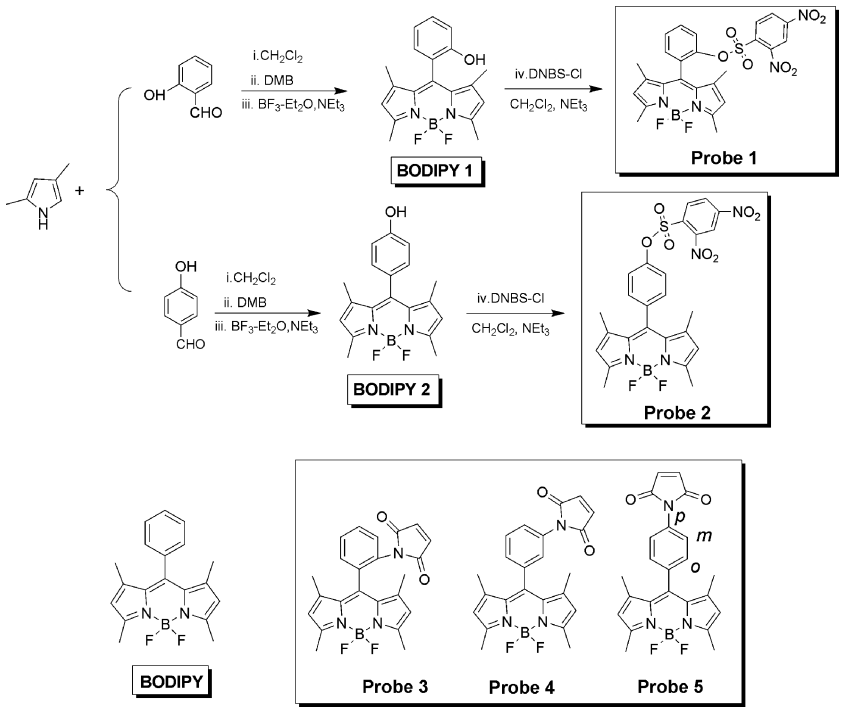

Scheme 1 Synthesis of the BODIPY-based thiol probes **1** and **2**. The known thiol probes **3**, **4** and **5** are presented for comparison (note **4** and **5** cannot be used as probes due to significant background emission, *i.e.* the non-efficient PET effect).[7]

the BODIPY core and the maleimide unit, which ensures efficient PET. The electron donor/acceptor distances in **4** and **5** are much larger than that of probe **3**. Thus the PET effect is not efficient in probe **4** and **5**. These results indicate that maleimide is not a strong electron acceptor relative to BODIPY for the assembly of PET fluorescence OFF–ON molecular probes. This postulation is supported by another Ru(II) bispyridine complex/maleimide thiol probe which also shows background emission (Φ = 0.036, note the parent Ru(II) complex shows Φ of 0.06, thus the maximum emission enhancement of the Ru(II)-based thiol probe in this case will be only *ca.* 2-fold).[8] These results indicate that maleimide is not a *universal* electron acceptor for assembly of OFF–ON PET probes.

To tackle this challenge, we set out to search for *more potent* electron acceptors than maleimide to assemble PET fluorescent probes, especially with *electron-deficient fluorophores* as photo-excited electron donors, such as BODIPY, thus creating more redundancy for design of the molecular probes, *e.g.*, the PET quenching will be effective even with the *p*-substitution (*e.g.* the profile of probe **2** and dyad **5**, Scheme 1), not restricted to *o*-substitution (profile of probe **1** and probe **3**, Scheme 1).

Recently 2,4-dinitrobenzenesulfonyl (DNBS) was used for the design of selective thiol probes and reactive oxygen species (ROS).[15–17] We demonstrated that by attachment of DNBS to a fluorophore, the DNBS induces the dark state (S_1) of the photophysics of the fluorophore,[9] thus the emission is switched off. Cleavage of the DNBS will re-establish the radiative S_1 state of the fluorophore; as a result the emission is switched on.[9] Recently we extended this strategy to a *phosphorescent* OFF–ON thiol probe with a Ru(II) polypyridine complex as the luminophore.[18] However, these sensors usually give weak absorption in the visible region and low luminescence quantum yields.

In order to tackle the aforementioned limitation of the current thiol probes, herein we devised highly selective PET fluorescence OFF–ON thiol probes **1** and **2** with BODIPY as the fluorophore (photo-induced electron donor) and DNBS as the electron acceptor (Scheme 1). Probe **1** is devised with the *o*-substitution and probe **2** is with the *p*-substitution profile. We demonstrated that both probe **1** and **2** show the fluorescence OFF–ON switching effect in the presence of biologically related thiols such as cysteine, although probe **1** shows a much higher contrast ratio (300) than probe **2** (54). Compared to the previously reported thiol probes **3** and **5**, our results demonstrate that DNBS is a more potent electron acceptor than maleimide to assemble PET fluorescent OFF–ON probes with especially electron-deficient fluorophores such as BODIPY, naphthalimide, *etc*.[19] The fluorescence OFF–ON sensing mechanism of the probes was rationalized by theoretical calculations. The DFT/TDDFT calculations indicate the dark S_1 excited state for probes **1** and **2** but radiative S_1 excited state for the fluorophores, and DNBS is *ca.* 0.76 eV more potent to accept electrons than the maleimide moiety. The probes were used for fluorescent imaging of cellular thiols.

Experimental

Synthesis of BODIPY 1

2-Hydroxybenzaldehyde (0.75 g, 6.0 mmol) and 2,4-dimethylpyrrole (1.26 g, 13.2 mmol) were dissolved in CH_2Cl_2 (200 mL). Then several drops of trifluoroacetic acid were added, the mixture was stirred at room temperature for 10 h. After, a solution of tetrachlorobenzoquinone (1.35 g, 6.0 mmol) in CH_2Cl_2 (120 mL) was added. The mixture was stirred for 4 h. After the addition of triethylamine (18 mL, 0.13 mol), $BF_3{\cdot}Et_2O$

(18 mL, 0.15 mol) was added dropwise, which was cooled in an ice–water bath. The mixture was stirred for 2 h. The solvent was removed under reduced pressure and the residue was dissolved with CH_2Cl_2 (100 mL). Then the organic phase was washed with water (2 × 100 mL). The organic portion was collected and dried over anhydrous Na_2SO_4, then the solvent was removed under reduced pressure. The crude product was purified with column chromatography (silica gel, ethyl acetate/petroleum ether, 1 : 20, v/v). Deep red solid powder was obtained. Yield: 0.71 g, 35.0%. M.p. 211 °C. λ_{max} (MeOH/H_2O = 4 : 1): 500 nm, ε_{max}: 75 200 M^{-1} cm^{-1}. ^1H NMR (400 MHz, $CDCl_3$) δ (ppm) = 7.35 (t, 1H, J = 7.2 Hz), 7.01–7.11 (m, 3H), 5.99 (s, 2H), 5.24 (s, 1H), 2.54 (s, 6H), 1.50 (s, 6H); ^{13}C NMR (100 MHz, $CDCl_3$): δ 156.6, 152.61, 143.6, 135.6, 131.6, 129.4, 121.8, 121.8, 121.2, 116.8, 14.8, 13.9; HRMS (TOF-MS-ESI) calcd for ($[C_{19}H_{19}BF_2N_2O - H]^-$), 339.1480; Found, 339.1482.

Synthesis of probe 1

BODIPY **1** (100.0 mg, 0.3 mmol) was dissolved in 10 mL dry CH_2Cl_2. Then, adding 0.1 mL dry triethylamine to the solution, the mixture was stirred for 5 min. After that the solution of 2,4-dinitrobenzenesulfonyl chloride (235.0 mg, 0.9 mmol) in CH_2Cl_2 was added dropwise to the above mixture at 0 °C. The reaction mixture was stirred for 10 h at room temperature. The solvent was removed under vacuum and the crude product was subjected to column chromatography (silica gel, DCM/Petroleum ether, 1 : 5, v/v). Probe **1** was obtained as a deep red solid (26.0 mg, 16.0%). M.p. 214 °C. λ_{max} (MeOH/H_2O = 4 : 1): 509 nm, ε_{max}: 73 800 M^{-1} cm^{-1}. ^1H NMR (400 MHz, $CDCl_3$) δ (ppm) = 8.60 (br, 1H), 8.13–8.16 (dd, 1H, J = 4.0 Hz, J = 8.0 Hz), 7.70 (d, 1H, J = 8.0 Hz), 7.58–7.65 (m, 2H), 7.48 (t, 1H, J = 8.0 Hz), 7.29–7.31 (m, 1H), 5.96 (s, 2H), 2.41 (s, 6H), 1.48 (s, 6H); ^{13}C NMR (100 MHz, $CDCl_3$): δ 157.1, 150.8, 147.4, 143.4, 134.7, 133.9, 131.7, 131.2, 128.7, 127.6, 125.9, 125.4, 122.0, 121.3, 14.6, 14.3; HRMS (TOF-MS-ES) calcd for ($[C_{25}H_{21}BF_2N_4O_7S + Na]^+$), 593.1090; Found, 593.1103.

Synthesis of BODIPY 2

4-Hydroxybenzaldehyde (0.37 g, 3.0 mmol) and 2,4-dimethylpyrrole (0.63 g, 6.6 mmol) were dissolved in THF (90 mL). Then several drops of trifluoroacetic acid were added, and the mixture was stirred at room temperature for 10 h. A solution of 2,3-dichloro-5,6-dicyano-*p*-benzoquinone (0.68 g, 3.0 mmol) in THF (120 mL) was added. The mixture was stirred for 4 h. After the addition of triethylamine (9 mL, 0.08 mol), $BF_3{\cdot}OEt_2$ (9 mL, 0.08 mol) was added dropwise to the mixture, which was cooled in an ice–water bath. The mixture was stirred overnight, and the solvent was removed under reduced pressure. The residue was dissolved with CH_2Cl_2 (100 mL) and the solution was washed with 5% aqueous $NaHCO_3$ (100 mL) followed by water (2 × 100 mL). The organic layers were dried over anhydrous Na_2SO_4. The solvent was removed under reduced pressure. The crude product was purified with column chromatography (silica gel, CH_2Cl_2), 0.54 g red solid powder was obtained, yield: 53.0%. M.p. 203 °C. λ_{max} (MeOH/H_2O = 4 : 1): 498 nm, ε_{max}: 81 100 M^{-1} cm^{-1}. ^1H NMR (400 MHz, $CDCl_3$) δ (ppm) = 7.11 (d, 2H, J = 8.0 Hz), 6.93 (d, 2H, J = 8.0 Hz), 5.98 (s, 2H), 5.13 (s, 1H), 2.55 (s, 6H), 1.44 (s, 6H); ^{13}C NMR (100 MHz, $CDCl_3$): δ 156.5, 155.5, 143.4, 141.9, 132.0, 129.6, 127.5, 121.4, 116.3, 14.7; HRMS (TOF-MS-ESI) calcd for ($[C_{19}H_{19}BF_2N_2O$ - $H]^-$), 339.1480; Found, 339.1494.

Synthesis of probe 2

BODIPY **2** (100.0 mg, 0.3 mmol) was dissolved in dry CH_2Cl_2 (10 mL). Then dry triethylamine (0.1 mL) was added to the solution, and the mixture was stirred for 5 min. A solution of 2,4-dinitrobenzenesulfonyl chloride (235.0 mg, 0.9 mmol) in CH_2Cl_2 was added dropwise at 0 °C. The reaction mixture was stirred for 10 h at 50 °C. The solvent was removed under reduced pressure and the crude product was subjected to column chromatography (silica gel, DCM/Petroleum ether, 1 : 3, v/v). Probe **2** was obtained as an orange-red solid (102.0 mg, 59.7%). M.p. 209 °C. λ_{max} (MeOH/H_2O = 4 : 1): 501 nm, ε_{max}: 84 300 M^{-1} cm^{-1}. ^1H NMR (400 MHz, $CDCl_3$) δ (ppm) = 8.67 (d, 1H, J = 4.0 Hz), 8.46–9.49 (dd, 1H, J = 4.0 Hz, J = 8.0 Hz), 8.16 (d, 1H, J = 8.0 Hz), 7.37 (d, 2H, J = 8.0 Hz), 7.31 (d, 2H, J = 8.0 Hz), 5.99 (s, 2H), 2.53 (s, 6H), 1.32 (s, 6H); ^{13}C NMR (100 MHz, $CDCl_3$): δ 156.5, 151.3, 149.4, 149.3, 142.7, 139.2, 135.5, 134.0, 133.5, 131.3, 130.5, 126.4, 123.2, 121.9, 120.6, 14.8, 14.7. HRMS (TOF-MS-ES) calcd for ($[C_{25}H_{21}BF_2N_4O_7S + Na]^+$), 593.1090; Found, 593.1066.

X-Ray single crystal determination

Single-crystal X-ray diffraction data were obtained on a Bruker SMART APEX CCD diffractometer using graphite monochromated MoKa (λ = 0.71073 Å) radiation with the SMART and SAINT programs. The data were collected using the φ/ω scan mode and corrected for Lorentz and polarization effects, during data reduction with SHELXTL 97 software, the absorption effect was corrected for as well. Crystallographic data for the structural analyses have been deposited with the Cambridge Crystallographic Data Center (CCDC). CCDC reference numbers for BODIPY **1**, probe **1** and probe **2**, are CCDC 787588, 787590 and 787589, respectively.†

Fluorescent imaging of the cellular thiols

The NCI-H446 cells were incubated with PBS (phosphate buffered saline) at 37 °C in DMSO–PBS solution (1 : 200, v/v, pH 7) for 1 h. Then the cells were washed with PBS buffer three times, and the probe (20 μm, 0.4 : 200 DMSO/PBS, v/v, pH 7) was added and incubated at 37 °C for 10 min. After that, the fluorescence imaging was performed after washing the cells with PBS buffer three times. The luminescence imaging of the cells was obtained using a Nikon ECLIPSE-Ti confocal laser scanning microscope. The green emission was observed with 488 nm laser excitation. The offset value is '70', and the pinhole is 'medium'.

Computational details

The ground state structures of the sensors were optimized using density functional theory (DFT) with B3LYP functional and 6-31G(d) basis set (considered as gas phase). The excited state related calculations were carried out with the time dependent DFT (TDDFT), based on the optimized structure of the ground state. There are no imaginary frequencies in the frequency analysis of all

calculated structures. All these calculations were performed with Gaussian 09W.[20]

Results and discussion

Design and synthesis of the BODIPY-based thiol sensors

We envisioned that fluorescent OFF–ON PET thiol probes could be designed with DNBS as an electron acceptor and BODIPY as an electron donor/fluorophore.[9,18] Thus BODIPY/DNBS probes **1** and **2** were devised and expected to show a fluorescence OFF–ON effect in the presence of thiols (Scheme 1). To compare the electron-withdrawing capability of DNBS and maleimide, probe **2** was designed as *para*-substituted (Scheme 1), thus the PET efficiency of **2** and **5** can be directly compared by their background emission. A weaker electron acceptor cannot perturb the photophysics of BODIPY; the emission of BODIPY will not be efficiently suppressed. If probe **2** can give weaker background emission than **5**, then DNBS is a more potent electron acceptor than maleimide.

The syntheses of probes **1** and **2** are straight forward (Scheme 1). Firstly, phenolic BODIPY **1** and **2** were prepared.[14] Then reaction with DNBS-Cl gives **1** in 16.0% overall yield. Probe **2** was prepared with a similar approach (31.6% overall yield).

Single-crystal structures of probes 1 and 2

The single crystals of BODIPY **1**, and probes **1** and **2** were obtained by slow evaporation of solutions of the compounds in CH_2Cl_2. The single crystal structures are presented in Fig. 1. In BODIPY **1**, the 2-hydroxyphenyl attached at C7 takes a perpendicular geometry against the BODIPY core (90.1°). This is due to the steric hindrance imposed by the methyl groups at C4 and C9 positions of the dipyrromethane core. For probe **1** (Fig. 1b), the phenyl ring at the C7-position of the BODIPY core takes a dihedral angle of 72.4° toward the BODIPY core. The BODIPY fluorophore takes a co-planar geometry, which is essential for strong fluorescence. The nitro groups (–NO_2) on the phenyl ring take non-coplanar geometry toward the sulfonylphenyl ring to which the nitro groups are attached. The *o*-nitro takes a 36.2° dihedral angle and the *p*-nitro takes a 21.5° dihedral angle. The distortion is probably due to the steric hindrance between the nitro groups and the phenyl ring. Furthermore, the sulfonylphenyl ring takes a parallel geometry to the BODIPY core and the distance between the two subunits of probe **1** is 3.68 Å. Thus π–π stacking is possible for the molecules packed in the single crystal.[19]

The single crystal of probe **2** was also determined (Fig. 1c). No π–π stacking was found. The distortion between the phenyl ring and the BODIPY core is 75.4°. Distortions of 80.7° and 12.8° were found for the *o*- and *p*- nitro groups, respectively.

These single crystal structures unambiguously verified the molecular structures of the thiol probes. To the best of our knowledge, this is the first time that the single crystal structures of BODIPY-based fluorescent molecular thiol probes were determined.

Selective detection of thiols with probe 1

Firstly probe **1** was studied for selective detection of thiols such as cysteine. The UV-vis absorption spectra of the probe **1** before and after addition of cysteine are presented in Fig. 2a. Both precursor BODIPY **1** and probe **1** show similar absorption at 509 nm (Fig. 2a). The intense absorption is due to the $S_0 \rightarrow S_1$ transition of the BODIPY fluorophore, whereas the minor absorption at 350 nm may be due to the $S_0 \rightarrow S_2$ transition. The molar extinction coefficient (ε) at 509 nm is up to 73 800 M^{-1} cm^{-1}. This intense absorption of visible light is beneficial for fluorescence bioimaging

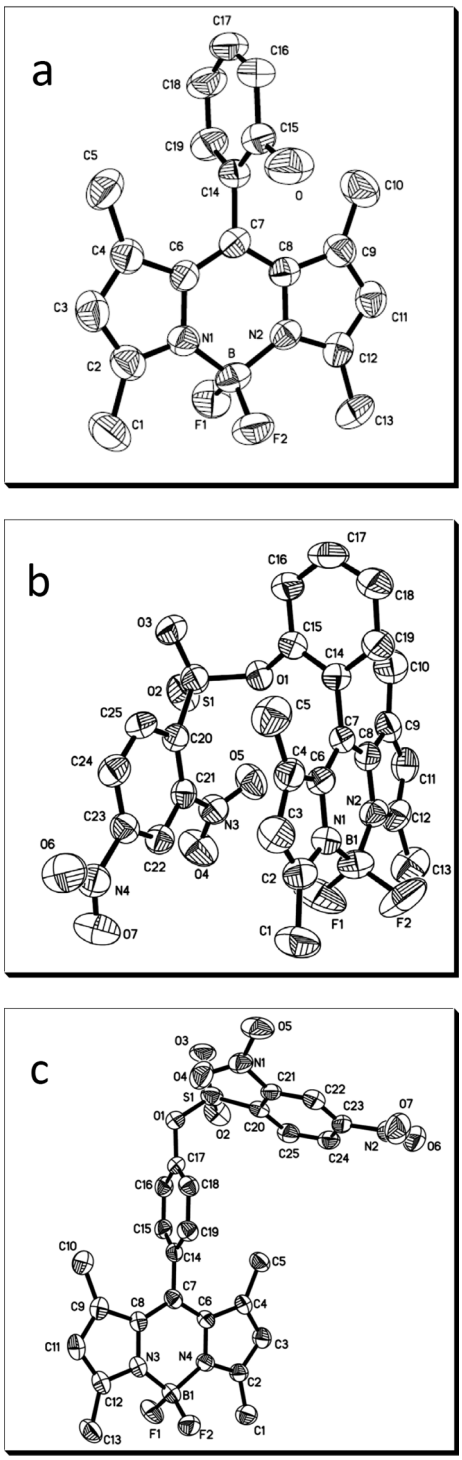

Fig. 1 ORTEP drawings of the compounds. (a) BODIPY **1**, (b) probe **1** and (c) probe **2**, with thermal ellipsoids shown at the 50% probability level. All H atoms are omitted for clarity.

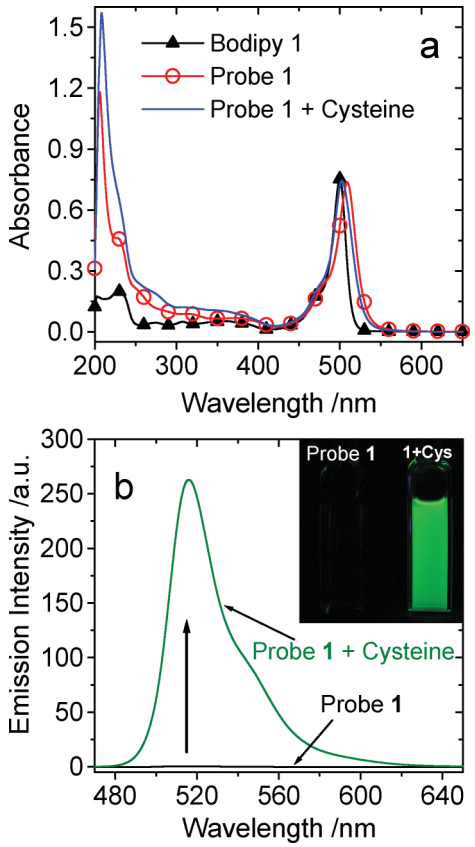

Fig. 2 (a) UV-vis absorption of BODIPY **1** and probe **1** before and after addition of L-cysteine. (b) Fluorescence emission spectra (λ_{ex} = 450 nm) of probe **1** before and after addition of L-cysteine. The fluorescence photos of the probe **1** alone and the mixture of probe **1**/cycsteine (incubated for 30 min) are also presented as the inset in (b). In MeOH/water (4/1, v/v) solution. At neutral pH, c (probe) = 1.0×10^{-5} mol L^{-1}, c (L-cysteine) = 2.0×10^{-3} mol L^{-1}. 20 °C.

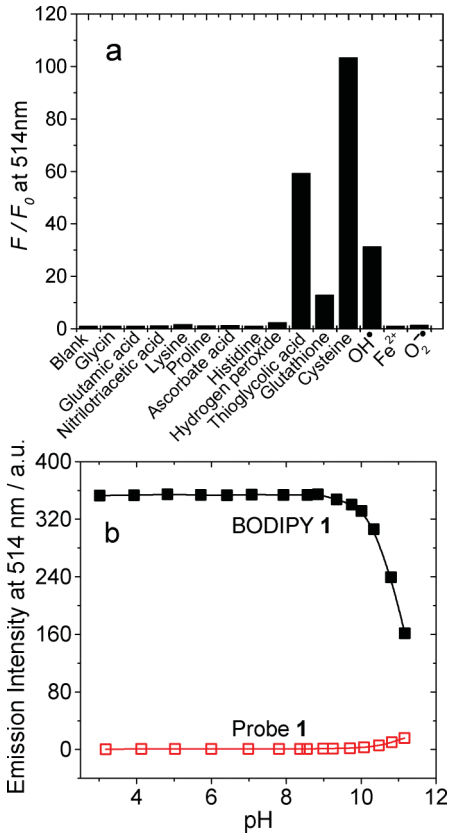

Fig. 3 Response of probe **1** to different analytes and pH. (a) Relative fluorescence intensity of 10 μM probe at 514 nm (λ_{ex} = 450 nm) before and after incubation in the presence of 2 mM analytes, incubated for 30 min at 37 °C. Neutral pH, in MeOH/water (4/1, v/v) solution. (b) The response of the emission of probe **1** and BODIPY **1** to the variation of pH. λ_{ex} = 503 nm. λ_{em} = 514 nm. $c = 1.0 \times 10^{-5}$ mol L^{-1}. 20 °C.

because without excitation in the UV region, the background fluorescence of the biological samples can be greatly suppressed. The similar UV-vis absorption of probe **1** and its precursor BODIPY **1** indicated that the Frank-Condon excited state of the BODIPY core is not perturbed by the introduction of DNBS, thus suggesting a supramolecular photochemical feature for the interaction between DNBS and BODIPY, *i.e.* there is no significant electronic communication between the BODIPY and the DNBS subunit at the ground state (S_0 state). With the addition of cysteine, the absorption band does not show significant variation (Fig. 2a).

Probe **1** is non-fluorescent in aqueous buffer (Φ = 0.002) (Fig. 2b). In the presence of cysteine, however, the emission at 516 nm was intensified by 300-fold (Φ = 0.470). Thus a fluorescent OFF–ON switching effect was achieved with probe **1**. The detection limit to cysteine reaches 4.0×10^{-7} mol L^{-1}. The sensing mechanism is most probably PET. Our later DFT/TDDFT calculations proved this speculation. Probe **1** is transformed into BODIPY **1** with cleavage of DNBS by thiols, thus the green emission will be switched on.[9,15–18] The proposed sensing mechanism was proved by mass spectrometry of the reaction mixtures (see the ESI†).

Other biologically related analytes were also tested against probe **1**. Glutathione induces positive responses (Fig. 3a). The sensing kinetics with glutathione are much slower than that with cysteine (see the ESI†).

The responses of probe **1** to ROS, such as $O_2^{-\bullet}$ and OH$^\bullet$ were also studied.[15b] We found that probe **1** gives a response to OH$^\bullet$ but not to $O_2^{-\bullet}$, which is different from a previously reported DNBS/fluorescein-based molecular probe for detection of superoxides.[15b]

Furthermore, the cleavage product of probe **1**, *i.e.* BODIPY **1**, can be ionized and the fluorescence of BODIPY **1** can be probably quenched. Thus the pH-dependencies of the emission of probe **1** and BODIPY **1** were also investigated (Fig. 3b). The results show that probe **1** is stable in the physiological pH range and the emission of BODIPY **1** is constant (the intensive emission is persistent) in the physiological pH range. To our knowledge, probe **1** is the only example of a thiol probe with BODIPY as an electron donor (*i.e.* d-PET) that shows fluorescent OFF–ON switching with green emission, except the previously reported probe **3**.[7]

Lower contrast ratio of OFF–ON probe 2: effect of the distance between electron donor/acceptor on the PET efficiency

The distance between the electron donor/acceptor in probe **2** is larger than that of probe **1**. This distance is tremendously important for the contrast ratio (or the PET efficiency) of the PET fluorescent molecular sensors. This is demonstrated by the

reported probes **3** and **5** (Scheme 1).[7] Probe **3** shows very weak background emission (Φ = 0.002, PET is efficient) but **5** shows undesired intense fluorescence (Φ = 0.54), due to the poor PET efficiency, which is believed to be caused by the larger distance between the electron donor and the electron acceptor.[7]

Probe **2** shows similar absorption at 501 nm (see the ESI†). Different from **5** (Φ = 0.54), probe **2** is very weakly fluorescent (Φ = 0.012) but shows drastically enhanced emission in the presence of thiols such as cysteine. The detection limit to cysteine is 4.9 × 10^{-6} mol L^{-1}, slightly lower than that of probe **1**. The cleavage product of probe **2** by thiols shows the intense BODIPY emission at *ca.* 512 nm (Φ = 0.283). Probe **2** is transformed into BODIPY **2** with cleavage of DNBS by thiols, thus the intrinsic photophysics of BODIPY are re-established and the green emission will be switched on.[9,15–18] The emission of probe **2** in the presence of thiols was intensified by 54-fold (Fig. 4a). This value is much smaller than that of probe **1**, which indicates that the PET efficiency of probe **2** is lower than that of probe **1**. The selectivity of probe **2** toward amino acids and biological thiols was also investigated (Fig. 4b). It was found probe **2** is highly selective toward cysteine. We found that the reaction of probe **2** with cysteine is faster than that with glutathione (see the ESI†). Probe **2** gives faster sensing kinetics than probe **1**, possibly due to the small steric hindrance of probe **2**.

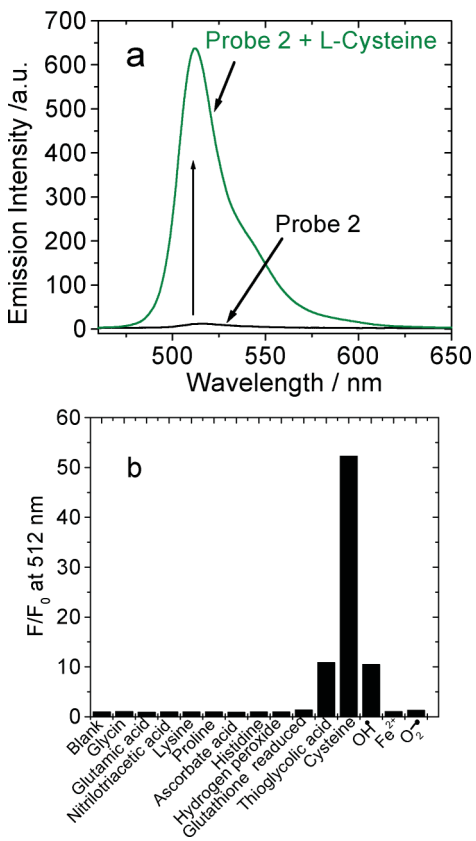

Fig. 4 (a) Fluorescence emission spectra (λ_{ex} = 450 nm) of probe **2** before and after addition of L-cysteine. (b) Relative fluorescence intensity of 10 μM probe **2** at 514 nm (λ_{ex} = 450 nm) before and after incubation in the presence of 2 mM analytes for 30 min. Neutral pH, in MeOH/water (4/1, v/v) solution. *c* (probe) = 1.0 × 10^{-5} mol dm^{-3}, *c*(L-cysteine) = 2.0 × 10^{-3} mol dm^{-3}. 20 °C.

Table 1 Photophysical properties of the BODIPY thiol probes and the BODIPY precursors

	λ_{Abs} (nm)/ε^a	λ_{ex}/nm	λ_{em}/nm	Φ^b
BODIPY 1	500/7.52 × 10^4	503	514	0.598
Probe 1	509/7.38 × 10^4	509	514	0.002
BODIPY 2	498/8.11 × 10^4	501	512	0.344
Probe 2	501/8.43 × 10^4	502	516	0.012
Probe 1+ L-cys	503/7.44 × 10^4	504	516	0.470
Probe 2+ L-cys	499/8.72 × 10^4	501	512	0.283

[a] Measurements were performed in solvent MeOH/water (4/1, v/v) and extinction coefficients ε (M^{-1} cm^{-1}) are also shown. [b] Luminescence quantum yields were measured with **BODIPY** (Scheme 1) as the reference (Φ = 0.48 in acetonitrile).[10b]

The main photophysical parameters of BODIPY-based probes **1** and **2** and the precursors are summarized in Table 1. We can see that probe **1** gives a much higher contrast ratio than probe **2**. We propose that this is due to the smaller distance between the electron donor and the electron acceptor. Compared to previously reported BODIPY-based thiol probes, such as **5** (Φ = 0.54), probe **2** is non-fluorescent.

Thus we propose that DNBS is a more potent electron acceptor than maleimide to construct PET OFF–ON fluorescent probes.

DFT/TDDFT calculations: elucidation of the fluorescence OFF–ON sensing mechanism and the electron accepting ability of DNBS

Recently theoretical calculations have been used for the study of the photophysics of fluorophores and fluorescent molecular probes.[21–24] Previously we used theoretical calculations based on density functional theory (DFT) and the time-dependent DFT (TDDFT) to study the d-PET effect of fluorescent boronic acid sensors,[25,26] as well as fluorescent OFF–ON thiol sensors.[9,18] The strategy we used in the rationalization of the fluorescence properties of the molecular sensors is to study the properties of the lowest-lying singlet excited state (S_1), which is responsible for the fluorescence emission (Kasha's rule).[27] The S_1 state will be a dark state if the oscillator strength of the $S_0 \rightarrow S_1$ transition is close to zero (forbidden transition). In this case the probe is non-fluorescent. Large oscillator strength indicates an allowed $S_0 \rightarrow S_1$ transition and the molecular probe is probably fluorescent.

The geometry of probe **1** was optimized with DFT methods. The geometry of the probe is similar to the single crystal structure (Fig. 1). For example, the optimized dihedral angle between the phenyl ring at the 7-position and the BODIPY core is 75.3°, which is very close to the 72.4° of the single crystal. The distortion of the *o*-nitro group toward the phenyl ring is 43.1°, close to the 36.2° of the single crystal.

Next, we studied the singlet excited states of the probes with the TDDFT calculations (Table 2). The excitation energy, oscillator strength (*f*) and the electronic composition of the singlet excited states are presented in Table 2. For probe **1**, we found that the S_1 state is a dark state.[24] Since transitions with complete charge transfer are forbidden, S_1 is a dark state, supported by the oscillator strength of $S_0 \rightarrow S_1$ (*f* = 0.0004); this means that probe **1** is non-fluorescent, which is in agreement with the experimental results (Fig. 2b). For the thiol-cleaved product, *i.e.* BODIPY **1**, however,

Table 2 Selected electronic excitation energies (eV) and oscillator strengths (f), configurations of the low-lying excited states of the probe **1** and the precursor BODIPY **1**, calculated by TDDFT//B3LYP/6-31G(d), based on the optimized ground state geometries

		TDDFT//B3LYP/6-31G(d)			
Compounds	Electronic transitions[a]	Excitation energy	f[b]	Composition[c]	CI[d]
Probe 1	$S_0 \rightarrow S_1$	1.84 eV (674 nm)	0.0004	H→L	0.7065
	$S_0 \rightarrow S_4$	2.96 eV (419 nm)	0.3694	H→L+2	0.4850
				H→ L+1	0.2393
				H–1→L	0.2246
BODIPY 1	$S_0 \rightarrow S_1$	3.02 eV (411 nm)	0.4704	H→L	0.5689
				H–1→L	0.1268
				H–2→L	0.1212

[a] Only selected excited states were considered. The numbers in parentheses are the excitation energy in wavelength. [b] Oscillator strength. [c] H stands for HOMO and L stands for LUMO. Only the main configurations are presented. [d] Coefficient of the wavefunction for each excitation. The CI coefficients are in absolute values.

the oscillator strength of the $S_0 \rightarrow S_1$ transition is 0.4704. This result indicates that $S_0 \rightarrow S_1$ transition is quantum mechanically allowed, as well as the $S_1 \rightarrow S_0$ transition. Thus, BODIPY **1** is probably fluorescent. This theoretical postulation is fully proved by experimental results (Fig. 2b).

In order to validate the aforementioned rationalization of the fluorescence OFF–ON mechanism of thiol probe **1**, the reported thiol probe **3** was also studied with the same approach and similar results was obtained, *i.e.* the BODIPY core serves as an electron donor and the maleimide subunit acts as the electron acceptor to constitute the dark S_1 state (see the ESI†).

The frontier molecular orbitals of probe **1** and the thiol cleaved product BODIPY **1** are presented in Fig. 5.

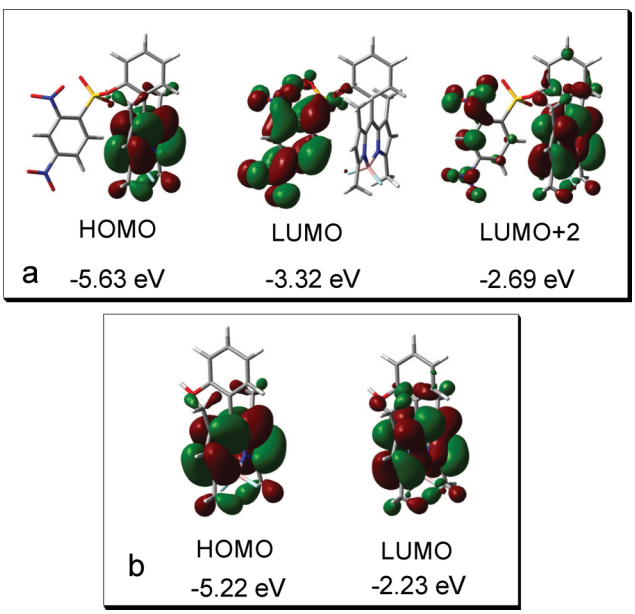

Fig. 5 The frontier molecular orbitals (MOs) of (a) probe **1** and (b) BODIPY **1** (*i.e.* the cleaved product of **1** by thiols). The energy levels of the MOs are shown (eV). Calculations are based on ground state geometry by DFT at the B3LYP/6-31G(d)/level using Gaussian 09.

This theoretical approach is applied to probe **2** and the precursor **2** (see the ESI†). Similar results were obtained compared to probe **1**. The HOMO of probe **2** is localized on BODIPY but the LUMO and LUMO+1 are located on DNBS, *i.e.* DNBS is an electron sink. However, the LUMO+2 of probe **2** is localized on BODIPY. The singlet excited states of probe **2** were studied with TDDFT calculations (see the ESI†). The HOMO→LUMO transition is involved in S_1. S_1 is a dark state, supported by the oscillator strength of $S_0 \rightarrow S_1$ (f = 0.0000), *i.e.* probe **2** is non-fluorescent.[8] This prediction was proved by experimental results. The main component of the allowed $S_0 \rightarrow S_5$ transition (f = 0.4708) of **2** is the BODIPY localized HOMO→LUMO+2. S_5 can be populated by direct photo-excitation, then *via* internal conversion the S_1 state is populated. However, $S_1 \rightarrow S_0$ is non-radiative. Therefore, the lack of emission of probe **2** is rationalized by the dark state S_1, which is induced by DNBS. More sophisticated computation was reported to rationalize the PET sensing mechanism;[24b] however, we propose that the DFT/TDDFT-based calculation is sufficient to predict the correct order of the dark excited state and the emissive excited state (Fig. 6).

With the same *p*-substituted profile, probe **5** (Scheme 1) shows undesired significant background emission (Φ = 0.54, thus it cannot be used as a fluorescent thiol probe), but probe **2**, with the same *p*-substituted scaffold, shows negligible background emission, thus probe **2** can potentially be used as a fluorescent thiol probe. Our results infer that DNBS is a more potent electron acceptor than maleimide because the *p*-substitution ensures effective PET for probe **2**, but for BODIPY–maleimide thiol probe **3–5** (Scheme 1), the PET is only effective with the *o*-substitution.[7] We set out to explain the different PET efficiency, or contrast ratio of probes **2** and **5** with theoretical calculations.

The optimization of **2** shows that the phenyl linker between BODIPY and DNBS takes a perpendicular geometry against BODIPY, thus there is no π-conjugation between BODIPY and DNBS moieties (the ESI†). This is corroborated by the similar UV-vis absorption of probe **1** and BODIPY (Fig. 2a). The energies of the HOMO are –5.44 eV and –5.33 eV for probes **2** and **5**, respectively (Fig. 6). TDDFT calculations indicate that the electron will be excited from H to L+2 or L+1 for probe **2** and **5**, respectively. Both L+2 and L+1 are originated from the BODIPY and have similar energies of –2.45 eV and –2.34 eV, respectively. The electron will relax to the unoccupied MOs with lower energy, such as L+1 and L for probes **2** and **5**, respectively. For **5**, the L (–2.97 eV) is localized on maleimide. For probe **2**, however, both

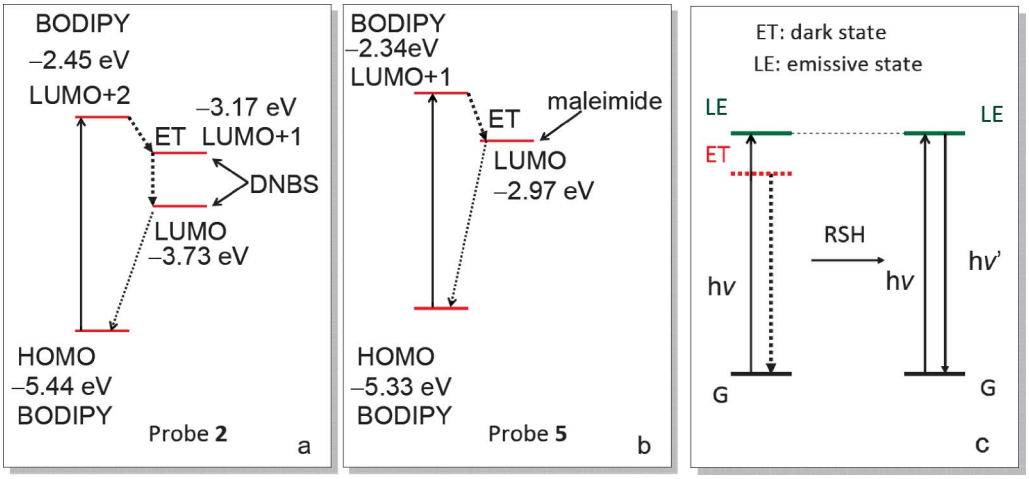

Fig. 6 Energy levels of the frontier molecular orbitals of (a) probe **2** and (b) probe **5**. The locations of the molecular orbitals are marked. DFT calculation is based on the ground state geometry at the B3LYP/6-31G(d) level using Gaussian 09. (c) Sensing mechanism of the probes **1** and **2** from an electronic excited state perspective. G stands for ground state, ET stands for electron transfer excited state (dark state) and LE stands for locally excited state (emissive state). Cleavage of the DNBS moiety will remove the dark state (ET) from the photophysics of the probe and thus emission will switch on.

L+1 and L are located on DNBS. Interestingly, the energy of the L of probe **2** is –3.73 eV, which is *ca.* 0.76 eV *lower* than maleimide in **5**. Thus, we propose DNBS is a *much more potent* electron acceptor than maleimide. Therefore, the background emission of probe **2** is much weaker than **5**. This is supported by the fluorescence quantum yields, *i.e.* $\Phi = 0.54$ for **5**,[7] *vs.* $\Phi = 0.012$ for probe **2**. Electrochemical measurements (cyclic voltammograms, *i.e.* CV, see the ESI†) corroborate these theoretical predictions. CV measurement of probe **2** indicate a reduction at more positive voltage (–890 mV, *i.e.* –3.53 eV) which is assigned to the DNBS moiety, whereas BODIPY shows the reduction at a more negative value (–1500 mV, *i.e.* 2.92 eV). Therefore, the DNBS disturbs the electronic structure of the BODIPY fluorophore. The ET dark excited state is beneath the bright state.[24b]

The driving force for PET can be evaluated with the free energy changes (ΔG°) derived from the Rehm-Weller equation (eqn (1)).[28–30] Where $E^\circ(D^+/D)$ is the oxidation potential of the electron donor, $E^\circ(A/A^-)$ is the reduction potential of the electron acceptor, herein the values are approximated as the energy difference of HOMO and LUMO (calculated with DFT). $\Delta E_{0,0}$ is the zero-zero transition energy (approximated as the crossing point of the excitation and the emission spectra of the sensors). w_p was not considered in the calculation of the ΔG° values. ΔG° of probes **2** and **5** was approximated as –0.76 eV and –0.11 eV, respectively. The much larger ΔG° of probe **2** than **5** indicates that DNBS is a more potent electron acceptor than maleimide. This finding will be helpful for the design of fluorescent molecular probes with more distinct OFF–ON switching abilities.

$$\Delta G^\circ = E^\circ(D^+/D) - E^\circ(A/A^-) - \Delta E_{0,0} + w_p \quad (1)$$

In vivo fluorescent imaging with probe 1 and 2

Fluorescent imaging of intracellular thiols with probe **1** was carried out (Fig. 7). The NCI-H446 cells were incubated with probe **1** and intense green emission was observed (Fig. 7d). In order to prove that probe **1** is specific to intracellular thiols, we used

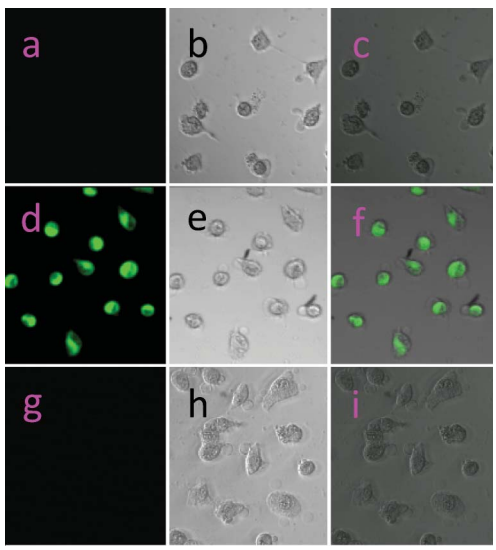

Fig. 7 Fluorescence images of NCI-H446 cells. (a) Fluorescence image of cell; (d) fluorescence image of cells incubated with probe **1** (20 μM) for 10 min; (g) fluorescence images of cells pre-treated with *N*-methylmaleimide (0.5 mM) for 1 h and then incubated with probe **1** (20 μM) for 10 min; (b, e, h) are the corresponding bright field images of (a, d, g); (c), (f) and (i) are the overlays of the respective fluorescent and bright images. 37 °C.

N-methylmaleimide to pre-treat cells to remove the intracellular thiols, then the cells were incubated with probe **1**, and no green fluorescence was observed (Fig. 7g).[9,18]

Probe **2** was also tested for fluorescent imaging of the cellular thiols. Green fluorescence emission was observed (see the ESI†). Interestingly, the green fluorescence emission is persistent even with pre-treatment of the cells with *N*-methylmaleimide.[9,18] This result indicates that, different from probe **1**, probe **2** can be cleaved by an unknown intracellular species, probably enzymes. Thus the *N*-methylmaleimide cannot inhibit the cleavage of DNBS from

probe **2**. Our result demonstrated that the regioisomers probe **1** and probe **2** show different intracellular specificities.

Conclusions

In conclusion, we have synthesized two new fluorescent OFF–ON green-emitting thiol probes **1** and **2** based on BODIPY/2,4-dinitrobenzenesulfonyl (DNBS) dyads. Probe **1** has the *o*-substituted phenyl scaffold and probe **2** has the *p*-substitution profile, thus the electron donor/electron acceptor distance of probe **2** is larger than that of probe **1**. This different electron donor/acceptor distance may impose a significant effect on the contrast ratio (PET efficiency) of the probes. Both probes show intense absorption at approximately 500 nm. Probe **1** is non-fluorescent. Cleavage of DNBS with thiols re-establishes the emissive S_1 state of BODIPY, up to 300-fold emission enhancement was observed. A similar result was observed for probe **2** but the emission enhancement decreased to 54-fold in the presence of cysteine. The higher contrast ratio of probe **1** than probe **2** indicates more efficient PET from BODIPY to DNBS for probe **1**, due to the smaller electron donor/acceptor distance. However, even with *p*-substitution, probe **2** is also a fluorescence OFF–ON thiol probe, which is in stark contrast to a previously reported BODIPY/maleimide dyad **5**, which shows significant background emission, due to the non-efficient PET from BODIPY to the maleimide subunit. Thus our results demonstrate that DNBS is a *more potent* electron acceptor than the well-established maleimide, by 0.76 eV based on DFT/TDDFT calculations. The sensing mechanism of the thiol probes was rationalized by DFT/TDDFT calculations, which indicate the dark S_1 excited state (oscillator strength $f = 0.0004$ for the $S_0 \rightarrow S_1$ transition) for probe **1** but the emissive S_1 state for the cleaved products (*i.e.* the BODIPY precursors of the probes, oscillator strength $f = 0.4704$ for the $S_0 \rightarrow S_1$ transition of BODIPY **1**). The probes **1** and **2** were used for fluorescent imaging of intracellular thiols. Probe **1** is specific for intracellular thiols (the green emission will be inhibited by *N*-methylmaleimide). For probe **2**, however, the green emission is persistent even with pretreatment of the cells with *N*-methylmaleimide. Our results show that DNBS is more potent than maleimide as an electron acceptor, this finding will be useful for assembly of fluorescent OFF–ON PET molecular probes, especially with *electron-deficient* fluorophores as the photo-excited electron donor, such as BODIPY. Furthermore, rationalization of the sensing mechanism of the molecular probes with DFT/TDDFT calculations will be useful for the design of fluorescent molecular sensors with predetermined photophysical properties.

Acknowledgements

We thank the NSFC (20972024 and 21073028), the Fundamental Research Funds for the Central Universities (DUT10ZD212), Ministry of Education (SRFDP-200801410004 and NCET-08-0077), the Royal Society (UK) and NSFC (China-UK Cost-Share Science Networks, 21011130154), State Key Laboratory of Fine Chemicals (KF0802), State Key Laboratory of Chemo/Biosensing and Chemometrics (2008009), the Education Department of Liaoning Province (2009T015) and Dalian University of Technology for financial support.

References

1 S. K. Kim, D. H. Lee, J. Hong and J. Yoon, *Acc. Chem. Res.*, 2009, **42**, 23.
2 A. T. Wright and E. V. Anslyn, *Chem. Soc. Rev.*, 2006, **35**, 14.
3 H. Refsum, A. D. Smith, P. M. Ueland, E. Nexo, R. Clarke, J. McPartlin, C. Johnston, F. Engbaek, J. Schneede, C. McPartlin and J. M. Scott, *Clin. Chem.*, 2004, **50**, 3.
4 J. Keelan, N. J. Allen, D. Antcliffe, S. Pal and M. R. Duchen, *J. Neurosci. Res.*, 2001, **66**, 873.
5 (*a*) X. Chen, Y. Zhou, X. Peng and J. Yoon, *Chem. Soc. Rev.*, 2010, **39**, 2120; (*b*) X. Chen, S. Ko, M. Kim, I. Shin and J. Yoon, *Chem. Commun.*, 2010, **46**, 2751; (*c*) Y.-B. Ruan, A.-F. Li, J.-S. Zhao, J.-S. Shen and Y.-B. Jiang, *Chem. Commun.*, 2010, **46**, 4938; (*d*) B. Zhu, X. Zhang, Y. Li, P. Wang, H. Zhang and X. Zhuang, *Chem. Commun.*, 2010, **46**, 5710; (*e*) B. Zhu, X. Zhang, H. Jia, Y. Li, H. Liu and W. Tan, *Org. Biomol. Chem.*, 2010, **8**, 1650; (*f*) B. Tang, L. Yin, X. Wang, Z. Chen, L. Tong and K. Xu, *Chem. Commun.*, 2009, 5293; (*g*) H. Li, J. Fan, J. Wang, M. Tian, J. Du, S. Sun, P. Sun and X. Peng, *Chem. Commun.*, 2009, 5904.
6 J. R. Lakowicz, *Principles of Fluorescence Spectroscopy*, 2nd ed.; Kluwer Academic/Plenum Publishers, New York, 1999.
7 T. Matsumoto, Y. Urano, T. Shoda, H. Kojima and T. Nagano, *Org. Lett.*, 2007, **9**, 3375.
8 J. Weh, A. Duerkop and O. S. Wolfbeis,, *ChemBioChem*, 2007, **8**, 122.
9 (*a*) S. Ji, J. Yang, Q. Yang, S. Liu, M. Chen and J. Zhao, *J. Org. Chem.*, 2009, **74**, 4855; (*b*) R. Zhang, X. Yu, Z. Ye, G. Wang, W. Zhang and J. Yuan, *Inorg. Chem.*, 2010, **49**, 7898.
10 (*a*) G. Ulrich, R. Ziessel and A. Harriman, *Angew. Chem., Int. Ed.*, 2008, **47**, 1184; (*b*) Y. Gabe, Y. Urano, K. Kikuchi, H. Kojima and T. Nagano, *J. Am. Chem. Soc.*, 2004, **126**, 3357.
11 S. C. Dodani, Q. He and C. J. Chang, *J. Am. Chem. Soc.*, 2009, **131**, 18020.
12 X. Peng, J. Du, J. Fan, J. Wang, Y. Wu, J. Zhao, S. Sun and T. Xu, *J. Am. Chem. Soc.*, 2007, **129**, 1500.
13 X. Zhang, Y. Xiao and X. Qian, *Angew. Chem., Int. Ed.*, 2008, **47**, 8025.
14 (*a*) A. Coskun, E. Deniz and E. U. Akkaya, *Org. Lett.*, 2005, **7**, 5187; (*b*) Y. Kubo, Y. Minowa, T. Shoda and K. Kimiya Takeshita, *Tetrahedron Lett.*, 2010, **51**, 1600.
15 (*a*) J. Bouffard, Y. Kim, T. M. Swager, R. Weissleder and S. A. Hilderbrand, *Org. Lett.*, 2008, **10**, 37; (*b*) H. Maeda, K. Yamamoto, Y. Nomura, I. Kohno, L. Hafsi, N. Ueda, S. Yoshida, M. Fukuda, Y. Fukuyasu, Y. Yamauchi and N. Itoh, *J. Am. Chem. Soc.*, 2005, **127**, 68; (*c*) X. Li, S. Qian, Q. He, B. Yang, J. Li and Y. Hu, *Org. Biomol. Chem.*, 2010, **8**, 3627; (*d*) S.-P. Wang, W.-J. Deng, D. Sun, M. Yan, H. Zheng and J.-G. Xu, *Org. Biomol. Chem.*, 2009, **7**, 4017.
16 H. Maeda, H. Matsuno, M. Ushida, K. Katayama, K. Saeki and N. Itoh, *Angew. Chem., Int. Ed.*, 2005, **44**, 2922.
17 W. Jiang, Q. Fu, H. Fan, J. Ho and W. Wang, *Angew. Chem., Int. Ed.*, 2007, **46**, 8445.
18 S. Ji, H. Guo, X. Yuan, X. Li, H. Ding, P. Gao, C. Zhao, W. Wu, W. Wu and J. Zhao, *Org. Lett.*, 2010, **12**, 2876.
19 (*a*) E. B. Veale, G. M. Tocci, F. M. Pfeffer, P. E. Krugera and T. Thorfinnur Gunnlaugsson, *Org. Biomol. Chem.*, 2009, **7**, 3447; (*b*) E. B. Veale, D. O. Frimannsson, M. Lawler and T. Gunnlaugsson, *Org. Lett.*, 2009, **11**, 4040.
20 M. J. Frisch, G. W. Trucks, H. B. Schlegel, G. E. Scuseria, M. A. Robb, J. R. Cheeseman, G. Scalmani, V. Barone, B. Mennucci, G. A. Petersson, H. Nakatsuji, M. Caricato, X. Li, H. P. Hratchian, A. F. Izmaylov, J. Bloino, G. Zheng, J. L. Sonnenberg, M. Hada, M. Ehara, K. Toyota, R. Fukuda, J. Hasegawa, M. Ishida, T. Nakajima, Y. Honda, O. Kitao, H. Nakai, T. Vreven, J. A. Montgomery, Jr., J. E. Peralta, F. Ogliaro, M. Bearpark, J. J. Heyd, E. Brothers, K. N. Kudin, V. N. Staroverov, R. Kobayashi, J. Normand, K. Raghavachari, A. Rendell, J. C. Burant, S. S. Iyengar, J. Tomasi, M. Cossi, N. Rega, J. M. Millam, M. Klene, J. E. Knox, J. B. Cross, V. Bakken, C. Adamo, J. Jaramillo, R. Gomperts, R. E. Stratmann, O. Yazyev, A. J. Austin, R. Cammi, C. Pomelli, J. Ochterski, R. L. Martin, K. Morokuma, V. G. Zakrzewski, G. A. Voth, P. Salvador, J. J. Dannenberg, S. Dapprich, A. D. Daniels, O. Farkas, J. B. Foresman, J. V. Ortiz, J. Cioslowski and D. J. Fox, *GAUSSIAN 09 (Revision A.1)*, Gaussian, Inc., Wallingford, CT, 2009.
21 F. Han, L. Chi, X. Liang, S. Ji, S. Liu, F. Zhou, Y. Wu, K. Han, J. Zhao and T. D. James, *J. Org. Chem.*, 2009, **74**, 1333.
22 Y. Liu, J. Feng and A. Ren, *J. Phys. Chem. A*, 2008, **112**, 3157.
23 O. A. Borg, S. S. M. C. Godinho, M. J. Lundqvist, S. Lunell and P. Persson, *J. Phys. Chem. A*, 2008, **112**, 4470.

24 (*a*) G. Zhao, J. Liu, L. Zhou and K. Han, *J. Phys. Chem. B*, 2007, **111**, 8940; (*b*) T. Kowalczyk, Z. Lin and T. V. Voorhis, *J. Phys. Chem. A*, 2010, **114**, 10427.
25 X. Zhang, L. Chi, S. Ji, Y. Wu, P. Song, K. Han, H. Guo, T. D. James and J. Zhao, *J. Am. Chem. Soc.*, 2009, **131**, 17452.
26 X. Zhang, Y. Wu, S. Ji, H. Guo, P. Song, K. Han, W. Wu, W. Wu, T. D. James and J. Zhao, *J. Org. Chem.*, 2010, **75**, 2578.
27 B. Valeur, *Molecular Fluorescence: Principles and Applications*, Wiley-VCH Verlag GmbH, New York, 2001.
28 J. Cody, S. Mandal, L. Yang and C. J. Fahrni, *J. Am. Chem. Soc.*, 2008, **130**, 13023.
29 M. E. McCarroll, Y. Shi, S. Harris, S. Puli, I. Kimaru, R. Xu, L. Wang and D. J. Dyer, *J. Phys. Chem. B*, 2006, **110**, 22991.
30 H. Sunahara, Y. Urano, H. Kojima and T. Nagano, *J. Am. Chem. Soc.*, 2007, **129**, 5597.